

# **2019 LANL Experiments and Simulations in Support of Salt R&D**

## **Spent Fuel and Waste Disposition**

*Prepared for  
US Department of Energy  
Spent Fuel and Waste Science and Technology  
Milestone M3SF-19LA010303014*

*Los Alamos National Laboratory  
Hakim Boukhalfa, Eric Gultinan, Thom Rahn, Doug  
Weaver, Brian Dozier, Shawn Otto, Philip H. Stauffer*

*Sandia National Laboratories  
Melissa Mills, Kris Kuhlman, Ed Matteo, Courtney Herrick,  
Martin Nemer, Jason Heath, Yongliang Xiong, Carlos  
Lopez*

*Lawrence Berkeley National Laboratory  
Jonny Rutqvist, Yuxin Wu, Mengsu Hu*

**September 30, 2019  
LA-UR-19-29830**

**DISCLAIMER**

This information was prepared as an account of work sponsored by an agency of the U.S. Government. Neither the U.S. Government nor any agency thereof, nor any of their employees, makes any warranty, expressed or implied, or assumes any legal liability or responsibility for the accuracy, completeness, or usefulness, of any information, apparatus, product, or process disclosed, or represents that its use would not infringe privately owned rights. References herein to any specific commercial product, process, or service by trade name, trade mark, manufacturer, or otherwise, does not necessarily constitute or imply its endorsement, recommendation, or favoring by the U.S. Government or any agency thereof. The views and opinions of authors expressed herein do not necessarily state or reflect those of the U.S. Government or any agency thereof.

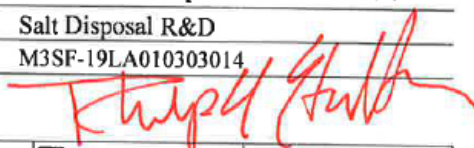


**FCT Quality Assurance Program Document**

**Appendix E  
FCT Document Cover Sheet**

**2019 LANL Experiments and  
Simulations in Support of Salt R&D**

Name/Title of Deliverable/Milestone  
Work Package Title and Number  
Work Package WBS Number  
Responsible Work Package Manager

**SF-19LA010303014**      **Salt Disposal R&D - LANL**  
1.08.01.03.03      Salt Disposal R&D  
Philip H. Stauffer      M3SF-19LA010303014  
(Name/Signature) 

Date Submitted

Quality Rigor Level for Deliverable/Milestone	<input checked="" type="checkbox"/> QRL-3	<input type="checkbox"/> QRL-2	<input type="checkbox"/> QRL-1 <input type="checkbox"/> Nuclear Data	<input type="checkbox"/> N/A*
-----------------------------------------------	-------------------------------------------	--------------------------------	-------------------------------------------------------------------------	-------------------------------

This deliverable was prepared in accordance with Los Alamos National Laboratory  
(Participant/National Laboratory Name)

QA program which meets the requirements of  
 DOE Order 414.1       NQA-1-2000

**This Deliverable was subjected to:**

Technical Review

**Technical Review (TR)**

**Review Documentation Provided**

- Signed TR Report or,
- Signed TR Concurrence Sheet or,
- Signature of TR Reviewer(s) below

**Name and Signature of Reviewers**

Thom Rahn

---



---

Peer Review

**Peer Review (PR)**

**Review Documentation Provided**

- Signed PR Report or,
- Signed PR Concurrence Sheet or,
- Signature of PR Reviewer(s) below



---



---

\*Note: In some cases there may be a milestone where an item is being fabricated, maintenance is being performed on a facility, or a document is being issued through a formal document control process where it specifically calls out a formal review of the document. In these cases, documentation (e.g., inspection report, maintenance request, work planning package documentation or the documented review of the issued document through the document control process) of the completion of the activity along with the Document Cover Sheet is sufficient to demonstrate achieving the milestone. QRL for such milestones may be also be marked N/A in the work package provided the work package clearly specifies the requirement to use the Document Cover Sheet and provide supporting documentation.

## EXECUTIVE SUMMARY

A borehole heater test conducted in the WIPP underground on pre-existing boreholes drilled in 2012 started in fiscal year 2018 continued into the first part of 2019. The testing focused on instrumentation design, development of sampling methodologies for gas and brine, and implementation of numerical methods to upgrade the FEHM code and add new functionalities. This document describes progress made in instrumentation design and modeling efforts to support the experimental design.

The examinations included several heating and cooling experiments performed to evaluate heating of the rock salt, brine migration into the heated borehole, and borehole permeability changes. Experimental data and modeling results consistently showed that a block heater was not able to transfer sufficient heat to the rock salt to achieve the desired temperatures targeted for the experiment. A modification of the packer heater assembly was necessary and the use of a radiative heater with 750 W was found appropriate. With the use of the radiative heater the target temperature of 120° C at the interior surface of the heated borehole was achieved and overall heating effect in rock salt was visible up to 1 meter away from the heater. The selection of this heater demonstrates the benefit of an iterative design process which relied on “ground truthing” equipment along with predictive numerical modeling.

Brine migration toward the heated borehole was measured during several cycles of heating and cooling experiments and numerical simulations were performed to validate the model using experimental data. The water production data were simulated successfully using a permeability of  $10^{-21}$  m<sup>2</sup> which suggests the lack of the presence of a higher permeability layer within the boreholes used for testing. Good agreement on water production and thermal response from FEHM and TOUGH-FLAC give the team confidence in their ability to simulate the experiments. Brine collection for chemical characterization of the brine inflows into the heated borehole was mostly unsuccessful. A design modification was needed and is being implemented in the larger heater test.

# CONTENTS

Contents.....	iv
LIST OF FIGURES.....	v
LIST OF TABLES .....	vii
Acronyms .....	vii
1. Background.....	1
2. Test Overview .....	2
2.1 Test location and testing goals .....	2
2.2 Borehole layout description .....	3
2.3 Heaters design and testing.....	5
2.4 Brine inflow characterization.....	6
2.5 Borehole closure measurement .....	6
2.6 Gas permeability measurements .....	7
2.7 Brine sampling and brine analysis .....	7
3. Description of Testing Performed and Initial Results .....	7
3.1 Design and testing of the heaters .....	7
3.2 Moisture collection .....	10
4. Modeling results .....	12
4.1 FEHM modeling .....	12
4.1.1 Model initialization and simulation .....	12
4.1.2 Variable temperature heater block simulations.....	14
4.1.3 Radiative heating experiments and simulations.....	15
4.1.4 Brine Availability.....	16
4.1.5 Permeability Testing of Phase 2 Boreholes .....	20
4.2 TOUGH-FLAC coupled THM modeling of the shakedown test.....	22
5. Summary.....	24
6. References .....	24

## LIST OF FIGURES

Figure 2.1 Waste Isolation Pilot Plant (WIPP) underground layout map showing the location of the existing boreholes used for shakedown testing.....	3
Figure 2.2: Configuration of existing boreholes used in phase 1 testing installation of an infrared heater in the WIPP underground.....	4
Figure 2.3 Schematic cross-section view of the borehole and instrumentation in the shakedown heater test.....	4
Figure 2.4 Schematic representation of the layout of the different boreholes instrumented in shakedown testing.....	5
Figure 2.5 Different heaters used during phase 1 shakedown testing. (a) stainless steel block heater powered with 1000 watt cartridge heater, (b) 260 watt heater lamp heater, (c) 750 watt heater lamp heater.....	5
Figure 2.6 Schematic diagram showing the shakedown test moisture collection and measurement systems.....	6
Figure 3.1 Temperatures recorded in the temperature borehole situated in the borehole to the north (adjacent) to the heater borehole. TB0 is the immediate location at the level of the heater at about 1 ft from the heater. The TBPX series are locations that are X ft. away/deeper in the borehole from TB0. The TBMX series are X ft. away/shallower from TB0. The data show temperatures in the formation induced by three different heaters tested.....	8
Figure 3.2 Simulations representing the temperature profiles in the heated borehole for the fully coupled and minimally coupled heating scenarios. Details of the simulations are presented in Section 4.....	9
Figure 3.3 Experimental data showing temperatures in the temperature borehole (TSB0) situated at about 2 inches from the heat source (see figure 4 for exact distance and locations) and temperatures in the small temperature borehole located 10.8" directly below the heat source (TSB0) along with the simulation considering full coupling between the heater and salt (SIM-TB0-fully coupled heater and SIM-TSB0-fully coupled heater) and simulations considering minimal coupling between the heater and salt.....	9
Figure 3.4 Projected temperature profiles using the 750 watt heater.....	10
Figure 3.5 Plot showing water extraction by nitrogen circulation through the isolated interval of the borehole.....	11
Figure 3.6 Water mass removal and numerical simulation for various experiments performed during shakedown testing.....	11
Figure 4.1 Cross-section of the model geometry, showing borehole in yellow, packer in orange, heater in red, the damaged rock zone in dark blue, and the background salt in light blue. The full mesh is 20 m × 10 m × 20 m and is composed of 1,003,995 elements.....	12
Figure 4.2 Cross-section of model domain parallel to drift face. A) 20m X 20m domain B) 3m X 3m subsection centered around the borehole.....	13
Figure 4.3 Brine pore pressure distribution development for shakedown simulation initialization.....	14
Figure 4.4 Final simulation of the 120 °C heater block experiment. Observations are black & gray, model predictions blue.....	15

Figure 4.5 A) Simulation of 260 W infrared heater and B) 750 W infrared heater experiment. ....	16
Figure 4.6 Water production during the 120 °C heater block and 260 W radiative heating experiment compared to simulations. Observations from desiccant are points while the simulations are represented by lines. ....	17
Figure 4.7 Initial saturation condition at the start of testing, 30 days after 750 W radiative heating, and 3 years of 750 W heating. The heater increases the nearby vapor pressure and drives the remaining saturation out of the nearby DRZ and intact salt. After approximately 1 year water begins to pool behind the nitrogen injection. ....	18
Figure 4.8 Long term water production during a 750 W radiative heating simulation of the shakedown test. Two linear trends are identified: an early trend, which is controlled by water sourced between the heater and the nitrogen source, and a late trend, which receives water from the entire borehole through ponded water which accumulates and reaches the nitrogen source. ....	19
Figure 4.9 A comparison of water production from a borehole with a saturated DRZ (freshly drilled) and one with the saturation profile of the shakedown simulation. ....	20
Figure 4.10 Permeability testing data compared to FEHM simulations of the heated borehole in the Phase 2 borehole configuration. The data is approximately matched with a permeability of $2e-17 \text{ m}^2$ . ....	22
Figure 4.11 Comparison of flow rate predicted during the 120 C steel block heater predicted by FEHM (left) and TOUGH-FLAC (right). TOUGH-FLAC data from <i>Rutqvist et al., 2019</i> . ....	23
Figure 4.12 Borehole closure due to 750W heating simulated using TOUGH-FLAC. Data from reference 19. ....	23

## LIST OF TABLES

Table 4.1 Key initial parameters used for the shakedown salt simulations .....	13
Table 4.2 A summary of the permeability tests conducted on the Phase 1 borehole configurations.....	21

## ACRONYMS

BATS	brine availability test in salt
CBFO	Carlsbad field office (DOE-EM WIPP office)
DOE	Department of Energy
DOE-EM	DOE Office of Environmental Management
DOE-NE	DOE Office of Nuclear Energy
DRZ	disturbed rock zone
ERT	electrical resistivity tomography
LANL	Los Alamos National Laboratory
LBNL	Lawrence Berkeley National Laboratory
LVDT	linear variable differential transformer
RH	relative humidity
SFWST	Spent Fuel & Waste Science & Technology (DOE-NE program)
SNL	Sandia National Laboratories
US	United States
WIPP	Waste Isolation Pilot Plant (DOE-EM site)
XRD	X-ray diffraction
XRF	X-ray fluorescence



This page is intentionally left blank.

# 1. Background

Permanent isolation of used nuclear fuel (UNF) in salt received significant interest and has been investigated through several testing campaigns in the U.S. and in Germany over several decades [1-7]. The disposal of nuclear waste in salt is particularly appealing because of the great advantage offered by salt as an impermeable and “dry” medium with self-sealing properties [8,9]. The amount of brine found in salt is usually very low and can vary between 0.01 to 0.50 wt. %. Brine is present either in discrete inclusions of few millimeters in size or smaller or is heterogeneously distributed between salt grains. In addition, rock salt contains accessory minerals (clays and sulfates), which can contain a significant amount of water [10,11]. Past studies have documented the mobilization of brine contained in salt under thermal gradients. It was found that gas-free fluid inclusions migrate toward a heat source, brine moves under a pressure gradient near an excavation, and that evaporation and condensation of vapor changes the porosity of the salt near the heat source. Uncertainties remain on the rate of brine generation near a heat source, the chemical composition of brine as it moves through salt towards the heat source, and the potential generation of corrosive acid vapors through the dehydration of accessory minerals (i.e, magnesium chloride) present in the brine. The current testing efforts were undertaken to regain hands on experience with experimentation in the underground at WIPP and to collect physicochemical data related to salt response to heating to better constrain numerical models that are used to predict brine availability in salt and to collect datasets that can be used to improve understanding of the constitutive and conceptual models applied to generic salt repository science. Initial testing performed during 2019 fiscal year used existing boreholes drilled in 2012 and focused on developing instrumentation and new approaches for brine and gas sample collection, characterization of salt permeability and porosity surrounding a borehole, and the effects of temperature on these processes in bedded salt. The initial testing also focused on fundamental code development in support of a larger heated borehole testing outlined in a 2018 test plan [12]. Testing outlined in this report is labeled as the “shakedown test”.

Shakedown testing of the approach described in the 2018 test plan [12] “shakedown test” started in fiscal year 2018 and continued to the first half of the 2019 fiscal year. In the first phase of the shakedown heater test, a packer heater assembly was designed and installed in an existing 4.75” borehole with supporting instruments installed in both the heated borehole and adjacent boreholes. The temperature of the heater borehole was monitored continually in the areas immediately surrounding the heater and the adjacent monitoring boreholes during alternating heating and cooling periods. Dry nitrogen was used to sweep the heated borehole and drive brine inflow to a downstream gravimetric moisture collection system. Borehole closure was monitored using a linear variable differential transformer (LVDT) based centralizer system emplaced in the borehole between the packer and the heater assembly. Characterization of changes in the rock salt permeability near the heated zone was measured by pressurizing the borehole interval behind the packer and observing transient pressure decay. The packer/heater design were described in our previous report [13]. The testing focused on refining the designs of the various instruments and the design of the larger Phase 1 testing. One of the main lessons learned from the shakedown test is that the block heater originally considered for the experiment was not able to transfer heat efficiently to the rock salt which required modification to the heater assembly and the replacement of the block heater by an infrared radiative heater (IR heater). The new heater was deployed and a

heating experiments run for several months. Brine generation data were collected before heating and during intermittent heating events performed with the block heater and with the IR heater. Modeling efforts were undertaken to upgrade the FEHM code and add new functionalities [14, <https://fehm.lanl.gov>]. Experimental results obtained during the different tests performed in the shakedown testing were used to develop and calibrate numerical models that were used to inform the design of the larger Phase 1 experiment.

This document describes the experiments performed in the shakedown testing outlined in the test plan described in 2018 report [12], and model validation and code development to add new functionality to porous flow simulator FEHM (14). This testing consisted of designing a borehole heater test, outfitting the borehole with instrumentation to enable the monitoring of temperature data and water/brine mobilization in the borehole under ambient temperature conditions and subsequent to a series of heating and cooling events. The document also describes how the shakedown experiments and feedback from modeling allowed the redesign of the heating element used to drive heating is salt and improve the performance of testing. The new heater design and specifications were adopted for the larger Phase 1 experiments and demonstrates the interplay between experiments and modeling.

## **2. Test Overview**

### **2.1 Test location and testing goals**

The testing performed in the first half of fiscal year 2019 as part of the shakedown test was performed in boreholes drilled in 2012 located in the E-140 drift near N-1050 (Figure 2.1). The overall goals of the testing were outlined in a 2012 test plan [12], more specifically, the testing performed during the first half of FY19 focused on testing instrumentation and layout in preparation for the larger Phase 1 testing. Testing efforts focused on: (1) optimization of the design of the heater assembly, (2) design and testing of a continuous moisture monitoring and gravimetric moisture collection system, (3) design and testing of a borehole permeability apparatus, (4) design and testing of an LVDT system for borehole deformation measurement, (5) implementation and testing of resistive tomography (6) collection and analysis of brine samples, (7) upgrade the FEHM code and add new functionalities to support the experimental design of the larger Phase 1 experiment. Progress and preliminary testing are described in the following sections.

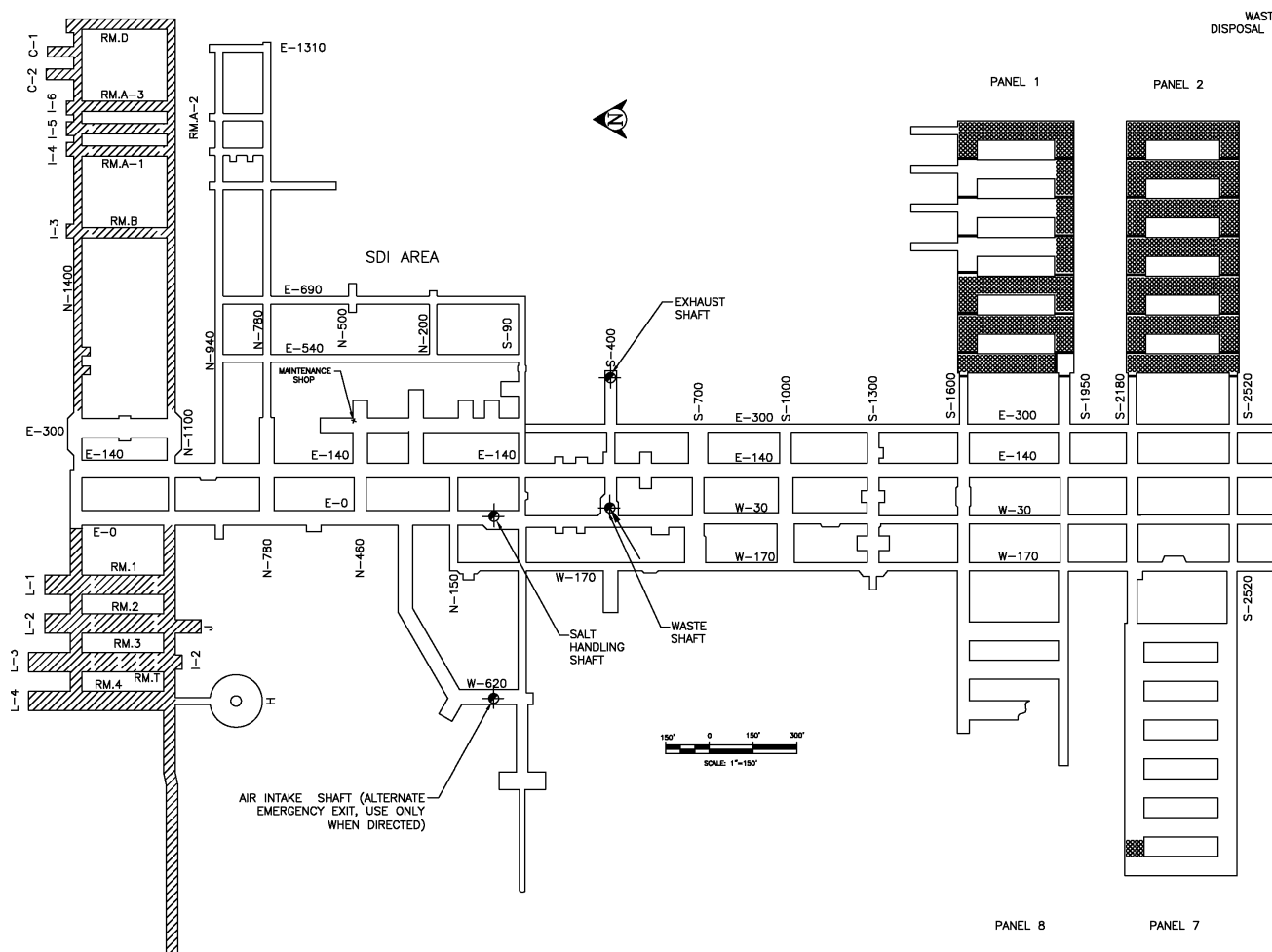


**Figure 2.1 Waste Isolation Pilot Plant (WIPP) underground layout map showing the location of the existing boreholes used for shakedown testing.**

## 2.2 Borehole layout description

The shakedown test was performed in existing boreholes drilled in 2018. The general layout and description of the instrumentation was reported in FY-18 report [13]. A figure of the boreholes before the instrumentation deployment and after the completion of the installation are shown in figure 2.2. The power supply box and other peripherals installed can be seen to the right of the existing boreholes.



**Figure 2.2: Configuration of existing boreholes used in phase 1 testing installation of an infrared heater in the WIPP underground.**

The main components of the packer heater assembly and instrumentation installed in the heated borehole are shown in the schematic representation depicted in figure 2.3.

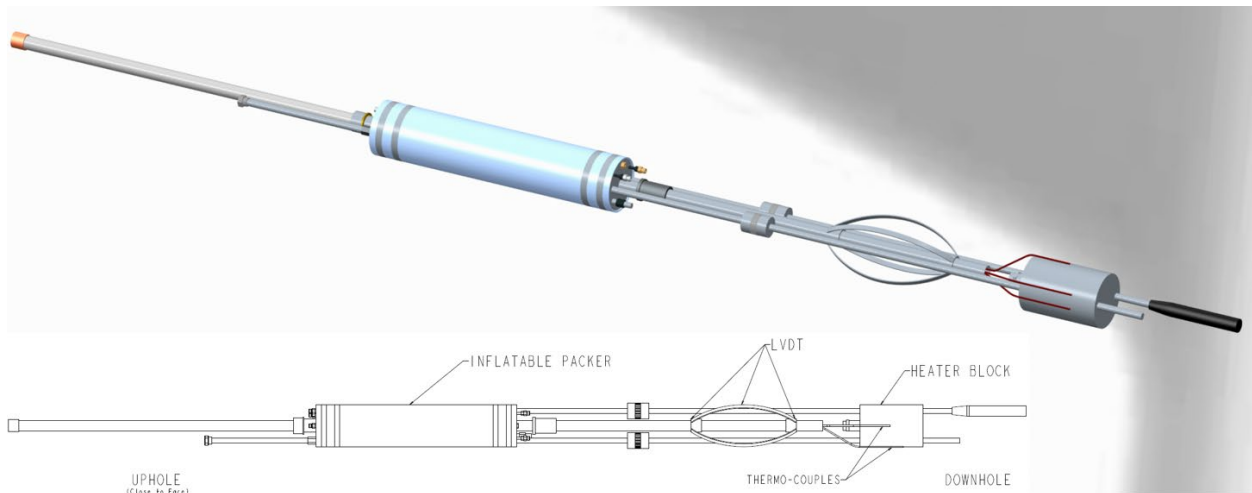


**Figure 2.3 Schematic cross-section view of the borehole and instrumentation in the shakedown heater test.**

The assembly includes a packer system used to isolate the back of the borehole from the drift area, an LVDT system designed to measure borehole closure, a heater assembly, thermocouples positioned along the heater assembly, a gas circulation line used to flow nitrogen gas behind the heater, and an access tube used to collect brine accumulated in the back of the borehole. The assembly was mounted on an access pipe used to mount the different components and allow the passage of the different power lines and thermocouples. The void space between the wires and the pipe was filled with an epoxy resin to seal the pipe and enable pressurization of the isolated area of the borehole for permeability testing. The front of the packer facing the drift was equipped with a pressure transducer connected to an access tube that allows reading of the pressure in the isolated area of the borehole. Thermocouples were also installed in two adjacent boreholes situated at 10.8" below the heated borehole and at 11.28" to the right of the heated borehole. The exact location of

the thermocouples relative to the heater is represented in the schematic diagram shown in figure 2.4.

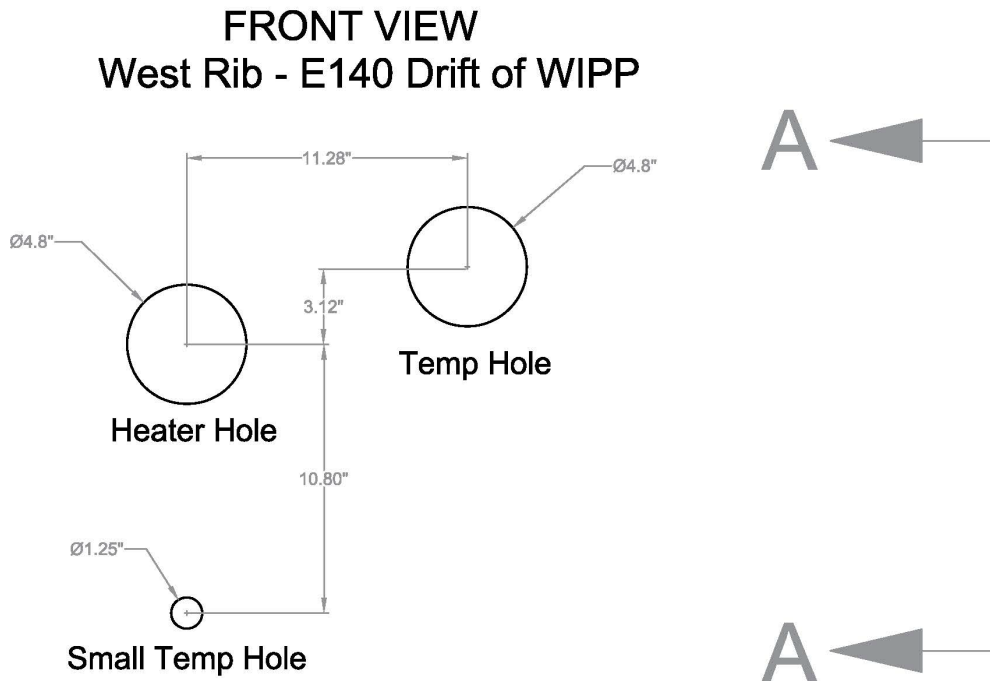


**Figure 2.4 Schematic representation of the layout of the different boreholes instrumented in shakedown testing.**

### 2.3 Heaters design and testing

Three separate heaters were used during the shakedown testing. The first heater was a stainless steel heater block equipped with a 1000 watt cartridge heater (Figure 2.5a), the second heater was a 260 helios quartz heater lamp (Figure 2.5b), and the third heater was a 750 watt helios quartz heater lamp (Figure 2.5c).



**Figure 2.5 Different heaters used during phase 1 shakedown testing. (a) stainless steel block heater powered with 1000 watt cartridge heater, (b) 260 watt heater lamp heater, (c) 750 watt heater lamp heater.**

A thermocouple reading the heater temperature was connected to a temperature controller used to power the heaters to a set temperature. Several heating and cooling experiments were performed during shakedown testing. The heater block and the 260 watt radiative heater lamp were found to be ineffective at heating the rock salt to the desired temperatures which required the use of a more powerful heater. The 750 watt heater was adopted for Phase 1 testing. More details of the testing are given in the preliminary results and modeling sections.

## 2.4 Brine inflow characterization

Characterization of brine inflow in the heated borehole was performed by reading the relative humidity of a nitrogen stream used to sweep the isolated area of the borehole under well-defined flow rate conditions. The nitrogen stream was also routed to a moisture capture system which allowed monitoring of the moisture contained in the nitrogen steam gravimetrically. A schematic representation of the setup is shown in figure 2.6.

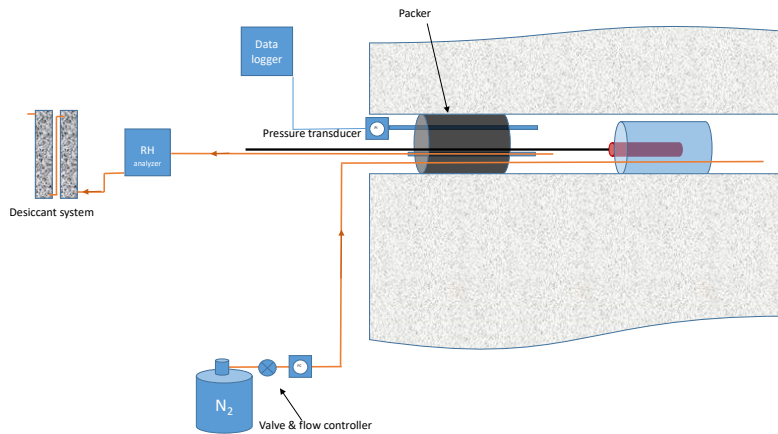


**Figure 2.6 Schematic diagram showing the shakedown test moisture collection and measurement systems.**

The desiccant cartridges were weighed regularly to determine mass gain due to moisture capture. The reading of the relative humidity probes and temperature was recorded continually and used to calculate the cumulative moisture driven through system. The flow rate was maintained constant at 200 mL/min throughout the experiment. Data obtained during the different heating and cooling testing phases will be presented in the results and modeling sections.

## 2.5 Borehole closure measurement

Borehole closure was monitored using a linear variable differential transformer (LVDT) system which was installed between the packer and the heater assembly (figure 2.3). The LVDT gauge measures changes in the diameter of the borehole through time. The gauge was designed based on a survey of downhole equipment used in the oil and gas industry and past experience with similar measurements that were made at both WIPP and Yucca Mountain. The LVDT gauge was built around a 1-inch Schedule 40 stainless steel pipe. Four bow springs were used to centralize the gauge. The bow springs are made of blue tempered AISI 1095 spring steel. Borehole deformation exerts a force on the bow springs which deforms and induces a sliding of the collar to which they

are attached. The movement of the sliding end collar was measured by a linear variable differential transformer (LVDT) and correlated to the deformation of the bow springs and used to determine the range of the borehole deformation. The LVDT design and calibration was described in our FY-18 report [13].

## **2.6 Gas permeability measurements**

Borehole permeability testing was performed by a series of pressurizations of the confined borehole area and observation of the pressure decay. The packer system was inflated to 50 PSI to isolate the borehole area behind the packer. The permeability testing is performed by pressurizing the confined borehole area to as high as 20 PSI and observing the pressure decay through a pressure gauge connected to a pass through pipe that connects to the confined area through the packer. The pressure readings were recorded using a data logger and processed numerically to determine the borehole permeability. Several permeability measurements were performed during the shakedown test for the existing heated borehole as well as for the newly developed boreholes drilled for Phase 1 testing. More details about the testing and numerical processing are presented in the results and numerical testing section. In general, we found it very difficult to perform these measurements. Developing a packer assembly with pass through cables devoid of leaks required several iterations of design and testing. The final design required fewer pass through wires and use of Conex compression fittings to achieve a leak free packer system adequate for permeability testing.

## **2.7 Brine sampling and brine analysis**

An access tube that allowed access to the back of the heated borehole was designed to allow brine sampling without the need to remove the packer assembly (Figure 2.3). The access tube was a 1/4 inch Teflon tube connected to a stainless steel pass through tube installed in the packer. The access tube allowed insertion of a 1/8 Teflon tube used during sampling to collect brine. This design was difficult to operate in practice and no brine was collected during the actual heating experiments. A new design was developed and is being tested in Phase 1 testing. Brine was collected by accessing the borehole after the removal of the packer. Brine was also collected in the newly drilled boreholes and analyzed for chemical composition.

# **3. Description of Testing Performed and Initial Results**

## **3.1 Design and testing of the heaters**

Several heating and cooling experiments were performed during shakedown testing. The initial testing was performed with the stainless steel heater (Figure 2.5a). The heater block temperature was set at a fixed temperatures of 120 °C and several heating and cooling cycles were run. The data in figure 3.1 (up to 12/16/18) show the profiles of the temperatures recorded on the heater and at several locations in the rock salt. As the data show, the temperature in the rock salt did not reach the desired temperatures predicted by the numerical simulations. Temperatures were recorded in the rock salt (Figure 3.4) in adjacent holes at about 1 ft from the heater and in line with the center of the heater. (+/- ~1.5 inches) Recorded temperatures changed only minimally (Fig. 3.4, TB0\_Avg). Temperatures recorded deeper in the temperature borehole (TBPX series) which are set at X ft deeper in the formation from the heater location are barely above ambient temperature.



Temperature in the formation moving towards the drift (TBMX\_Avg series) are also only slightly above ambient temperature.

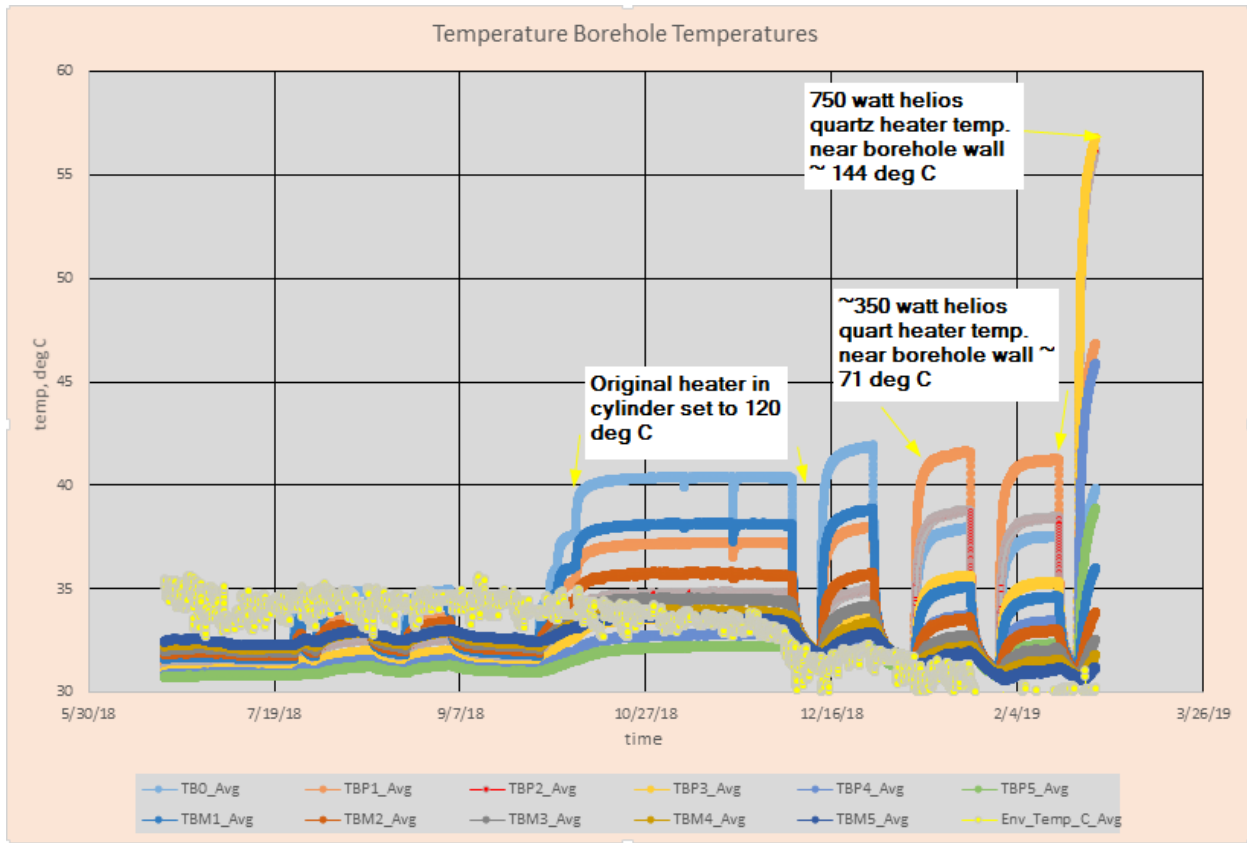


**Figure 3.1** Temperatures recorded in the temperature borehole situated in the borehole to the north (adjacent) to the heater borehole. TB0 is the immediate location at the level of the heater at about 1 ft from the heater. The TBPX series are locations that are X ft. away/deeper in the borehole from TB0. The TBMX series are X ft. away/shallower from TB0. The data show temperatures in the formation induced by three different heaters tested.

These results show that the block heater is not effective at supplying the designed heating potential. This is attributed to the low coupling between the heater and salt and to the air gap between the heater and salt, i.e. the air gap between the heater and the salt hinders efficient heat transfer (Figure 3.2). Numerical modeling performed on the results of the experiments show the contrast between the predicted and measured temperatures (Figure 3.3).

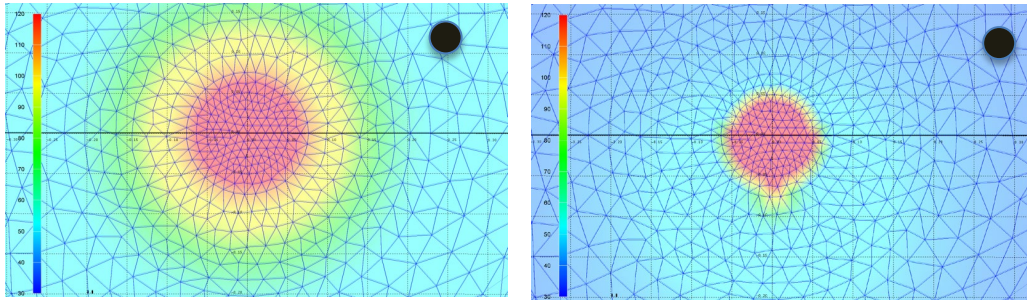


**Figure 3.2 Simulations representing the temperature profiles in the heated borehole for the fully coupled and minimally coupled heating scenarios. Details of the simulations are presented in Section 4.**

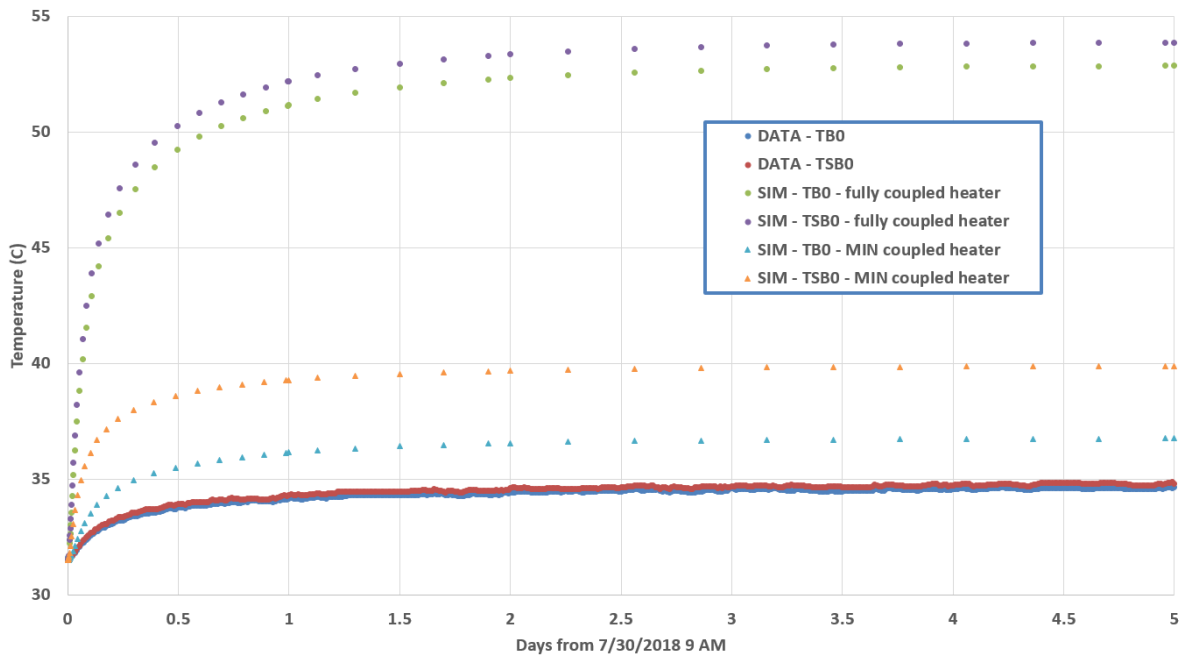


**Figure 3.3 Experimental data showing temperatures in the temperature borehole (TSB0) situated at about 2 inches from the heat source (see figure 4 for exact distance and locations) and temperatures in the small temperature borehole located 10.8" directly below the heat source (TSB0) along with the simulation considering full coupling between the heater and salt (SIM-TB0-fully coupled heater and SIM-TSB0-fully coupled heater) and simulations considering minimal coupling between the heater and salt.**

The details of the modeling are provided in Section 4. The simulations and experimental data suggest that the block heater might not be the best design needed to achieve the experimental goals, which are focused on inducing sufficient heating in salt to drive observable changes in its physiochemical properties. Radiative heaters were considered to test their ability to more effectively heat salt. Two different radiative heaters rated at 260 watt and 750 watt were tested.

The data in figure 3.1 show the temperature induced in the temperature borehole with the 260 watt heater and the 750 watt heater run at full power. The 260 watt heater was only slightly more effective than the block heater and was only able to heat the surface of the heated borehole to  $\sim 71$   $^{\circ}\text{C}$  at heater location and the temperature in the observation borehole to about  $42$   $^{\circ}\text{C}$ , which is still lower than the temperatures desired. The 750 watt heater improved performance and was able to create a sphere of heated salt with a gradient of temperature from  $140$   $^{\circ}\text{C}$  at the heater location to ambient temperature several feet away deeper in rock salt. Figure 3.4 shows a simulation for the projected temperatures in the rock salt in a 1 meter domain using a fully powered 750 watt heater. Details of the simulations are shown in Section 4. This radiative heater was adopted for further testing in the larger test planned for Phase 1.

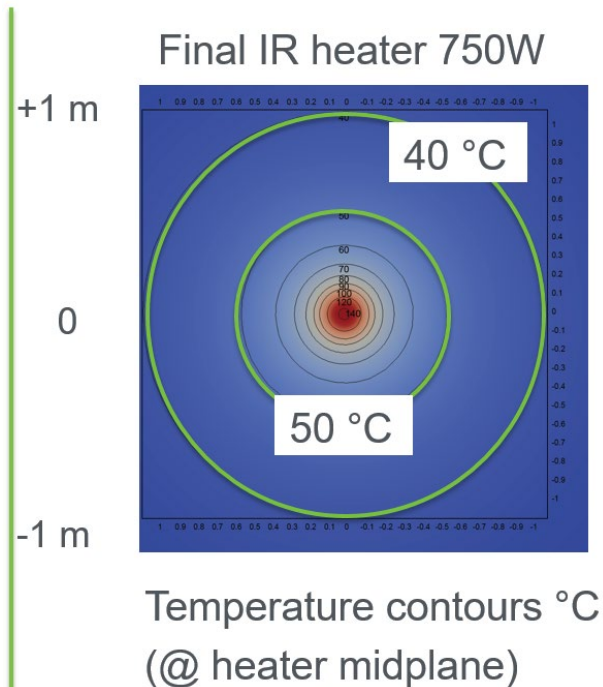


**Figure 3.4 Projected temperature profiles using the 750 watt heater.**

### 3.2 Moisture collection

Initial data from the gravimetric moisture collection data and of the relative humidity readings (RH) are summarized in figure 3.5. The RH plot decreases from about 50% at the start of the nitrogen flow and reaches a steady state at about 20%. This behavior was consistent for almost all the runs performed with the different heaters. The initial elevated RH is attributed to the presence of residual brine in the borehole and the presence of water adsorbed to the borehole walls. There is no apparent correlation between heating and brine inflow into the borehole. The rate of moisture accumulation in the desiccant cartridges was almost constant throughout the entire testing period and averaged 4.2 g/day. Brine inflow into the borehole is likely driven by the borehole rock salt permeability and brine inflow driven by the pressure of the formation. Details of the simulations and brine inflow simulations are presented in Section 4.

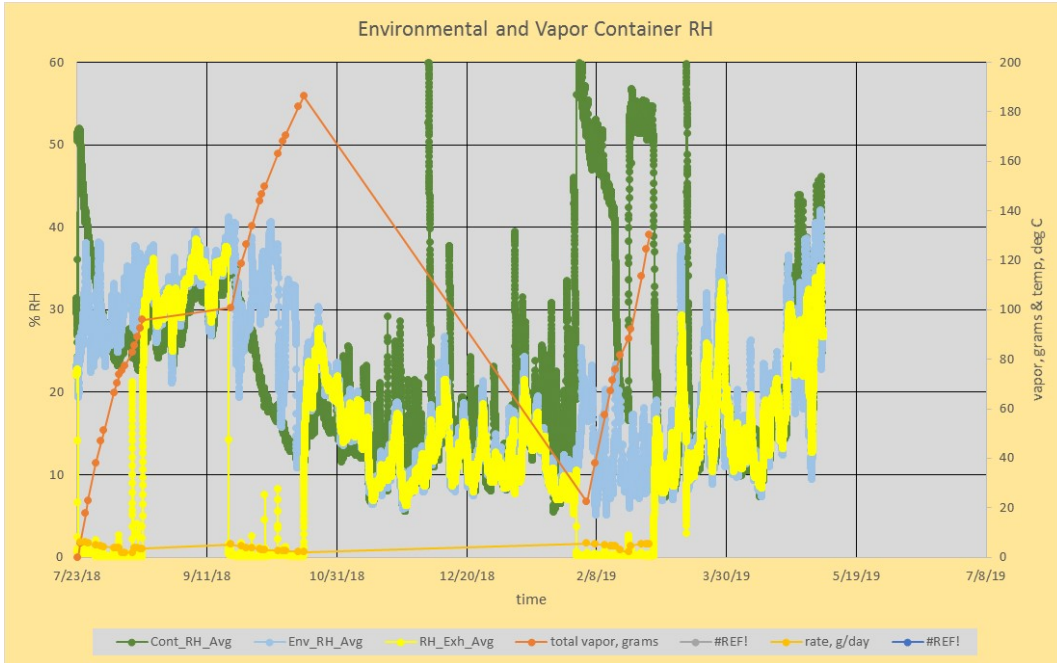


**Figure 3.5 Plot showing water extraction by nitrogen circulation through the isolated interval of the borehole.**

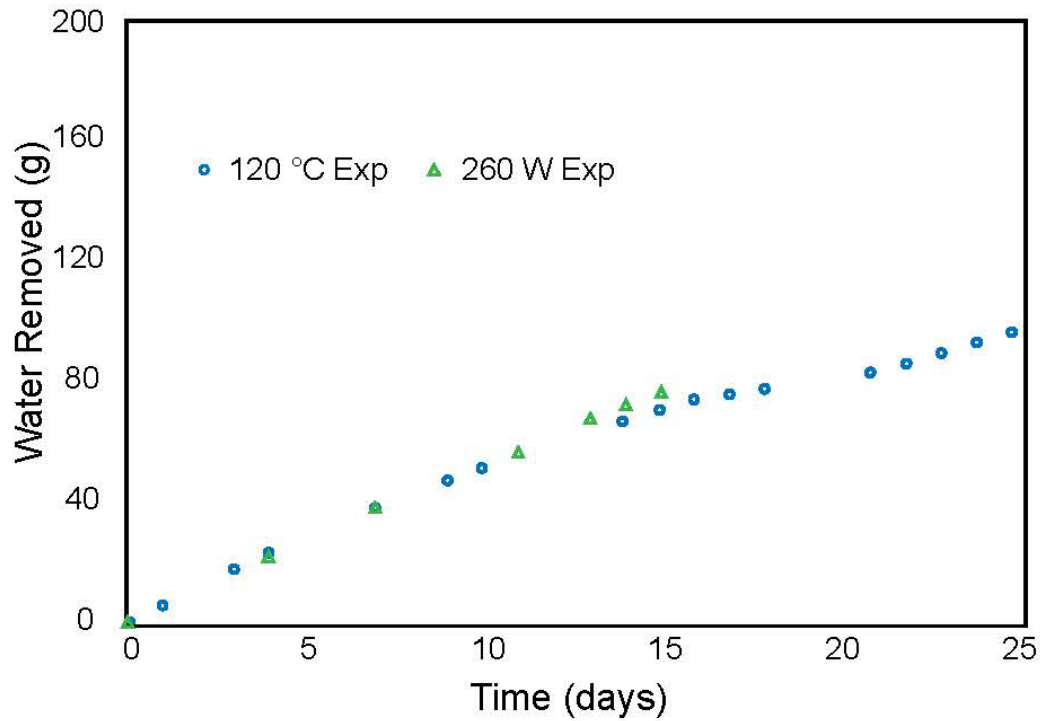


**Figure 3.6 Water mass removal and numerical simulation for various experiments performed during shakedown testing.**

## 4. Modeling results

### 4.1 FEHM modeling

#### 4.1.1 Model initialization and simulation

Model development at Los Alamos has been conducted using the porous flow simulator FEHM [14, <https://fehm.lanl.gov>]. To simulate the borehole heater experiments a three dimensional mesh was generated using LaGriT (<https://lagrit.lanl.gov>). The mesh is  $20\text{ m} \times 20\text{ m} \times 10\text{ m}$  (Figure 4.1, 4.2) with the center of borehole lying at  $x = 0, z = 0$ . The mesh is highly refined near the borehole and the resolution decreases radially. This results in a mesh of 1,003,995 elements. The high refinement near the borehole helps resolve high temperature, saturation, and pressure gradients near the borehole wall.

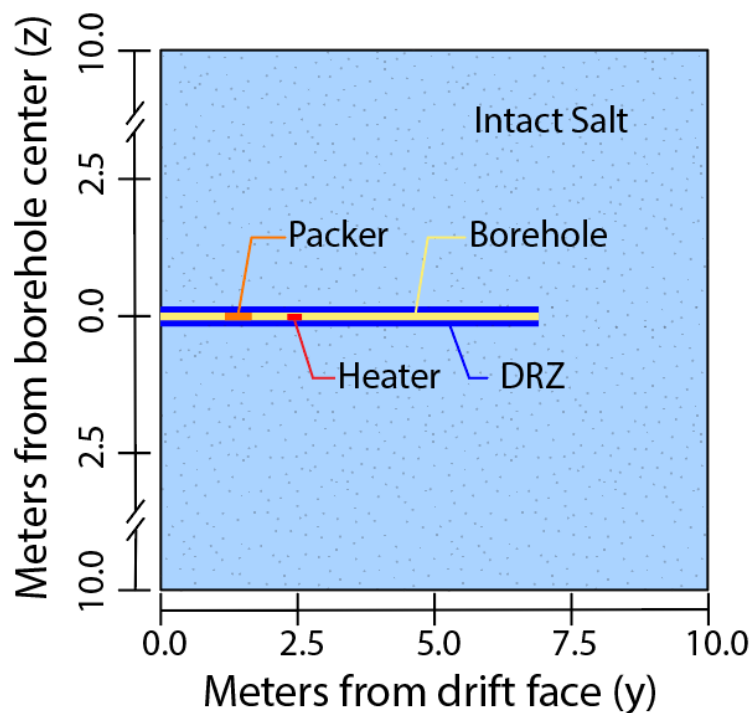


**Figure 4.1** Cross-section of the model geometry, showing borehole in yellow, packer in orange, heater in red, the damaged rock zone in dark blue, and the background salt in light blue. The full mesh is  $20\text{ m} \times 10\text{ m} \times 20\text{ m}$  and is composed of 1,003,995 elements.

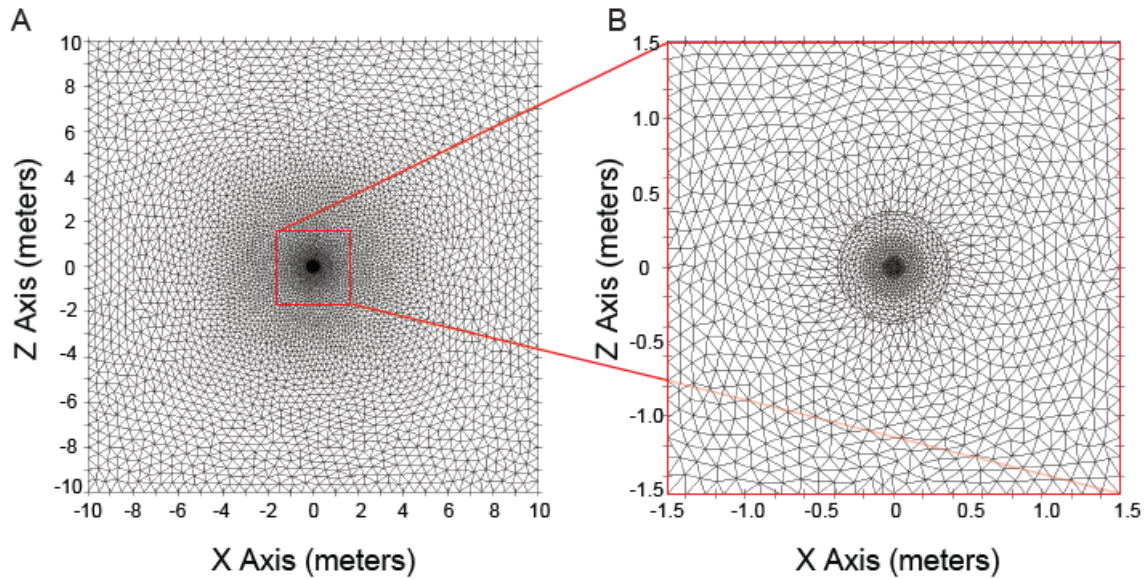


**Figure 4.2 Cross-section of model domain parallel to drift face. A) 20m X 20m domain B) 3m X 3m subsection centered around the borehole.**

Beginning with appropriate initial conditions is critical to model accuracy. Table 1 displays the initial properties of the intact and damaged rock zone salt used during the simulations. These properties are evolved during the simulation. For instance, porosity changes due to the dissolution of salt, which causes changes in permeability; whereas, temperature changes from the heater drive changes in thermal conductivity. The implementation of these coupled processes in FEHM has been developed over the past 8 years with many of the functions described in past reports and publications from our team [15-18].

**Table 4.1 Key initial parameters used for the shakedown salt simulations**

Parameter	Value
Salt initial porosity (-)	0.001
Salt initial permeability (m <sup>2</sup> )	10 <sup>-21</sup>
Damaged rock zone permeability (m <sup>2</sup> )	10 <sup>-18</sup>
Salt initial thermal conductivity (W/m K)	5.25
Initial formation pressure (MPa)	12
Initial formation temperature (°C)	31.5
Residual saturation (-)	0.1



Due to the extremely low permeability of intact salt, field measurements of formation pressure and saturation are difficult. Because salt cannot resist deviatoric stress, the far field formation pressure at WIPP should approach the lithostatic stress (15 MPa), however, experiments have shown that the formation pressure is likely less than the lithostatic stress and may be around 12 MPa [8,9]. Using this information and knowledge of the mining activities at WIPP we simulate an estimated pressure and saturation distribution at the location of the heated borehole in the E-140 drift. First, the model is initialized at 12 MPa throughout the domain, this represents the formation prior to the excavation of the mine (Figure 4.3). Next an atmospheric boundary condition is applied along one side, this represents the initial mining of the E-140 drift in 1982, and the model is allowed to equilibrate for 30 years. After 30 years of model time, the domain is further updated to include the borehole, this corresponds to the drilling of the boreholes in 2012. Next the model is run for an additional 6 years to arrive at the unsteady pressure and saturation condition within the formation at the start of the shakedown testing. These final distributions are then used as the initial pressure and saturation condition for each of the shakedown simulations.

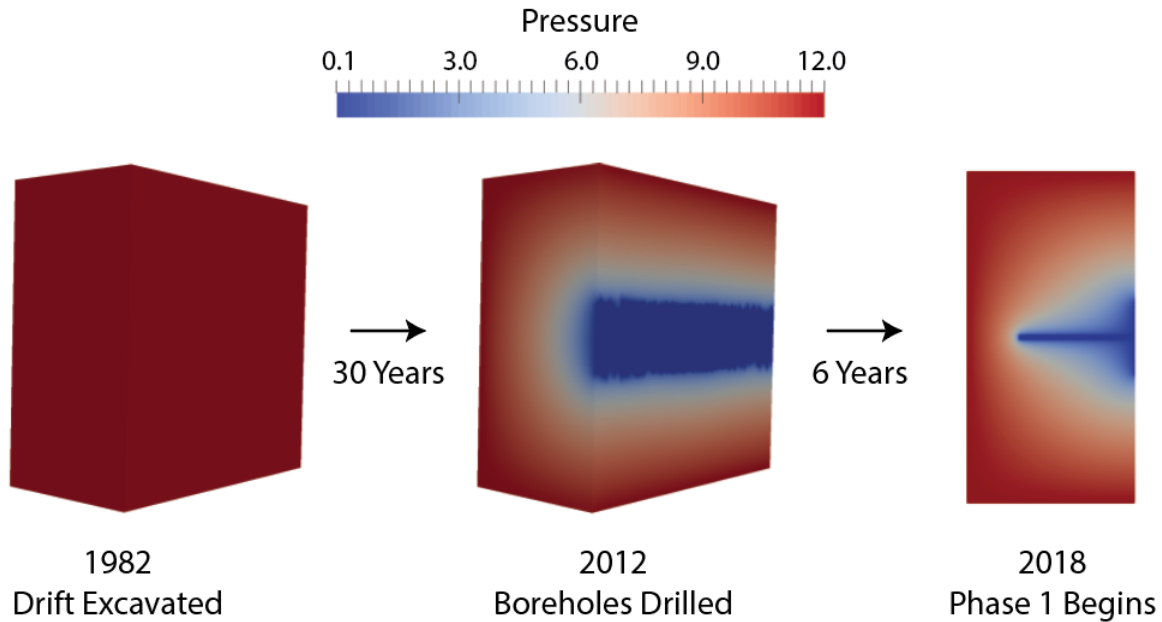


**Figure 4.3 Brine pore pressure distribution development for shakedown simulation initialization.**

#### 4.1.2 Variable temperature heater block simulations

Thermal properties of the formation salt can be determined through experimentation and modeling of time-dependent heat response to the heater in adjacent boreholes. Initial simulations of the shakedown experiment assumed full coupling between the heater and the borehole wall in the heated borehole. However, these preliminary simulations over-predicted the transfer of heat into the formation. To address the discrepancy between the simulated and measured temperature results, the simulations were modified to add an air gap around the heater in the heated borehole.

While the fully-coupled simulation assumed tight contact between the rock salt of the borehole wall and the heater, the minimally-coupled heater simulations assume only direct contact to the salt on the bottom of the heated borehole where the heater rests. This allows for thermal insulation around the heater due to the low thermal conductivity of air in the heated borehole. The final constant 120 °C shakedown heater simulation temperature results are shown in Figure 4.4. The model is able to represent the temperature at the monitoring locations to within 2 °C. Some error is likely associated with measuring the precise locations of the temperature sensors within boreholes. Each borehole is not perfectly straight and some movement of the temperature sensors during installation and grouting is possible.

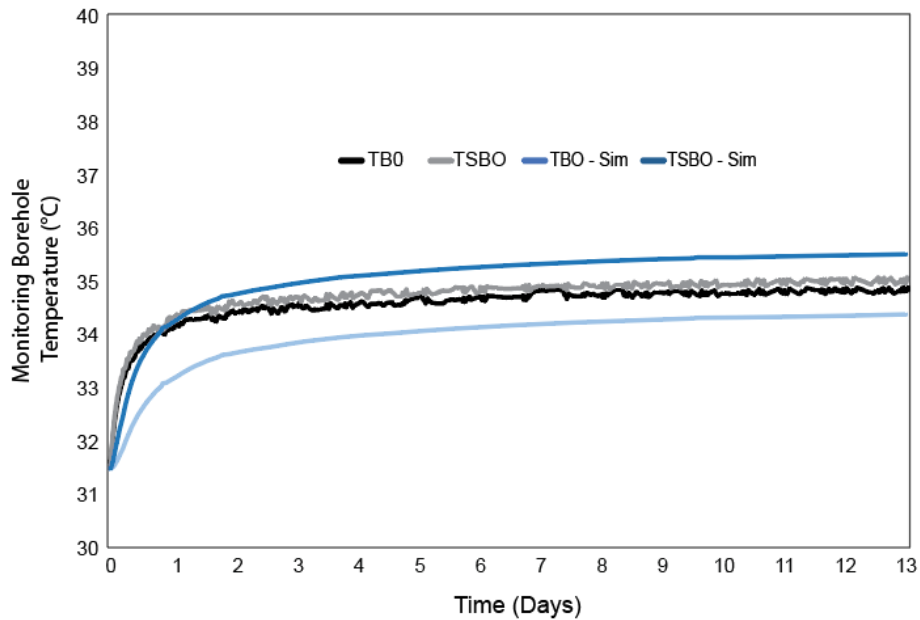


**Figure 4.4 Final simulation of the 120 °C heater block experiment. Observations are black & gray, model predictions blue.**

### 4.1.3 Radiative heating experiments and simulations

The radiative heating experiments are modeled using a fully coupled heater (no air gap), and a Neumann-style energy flux boundary condition (Figure 4.5).



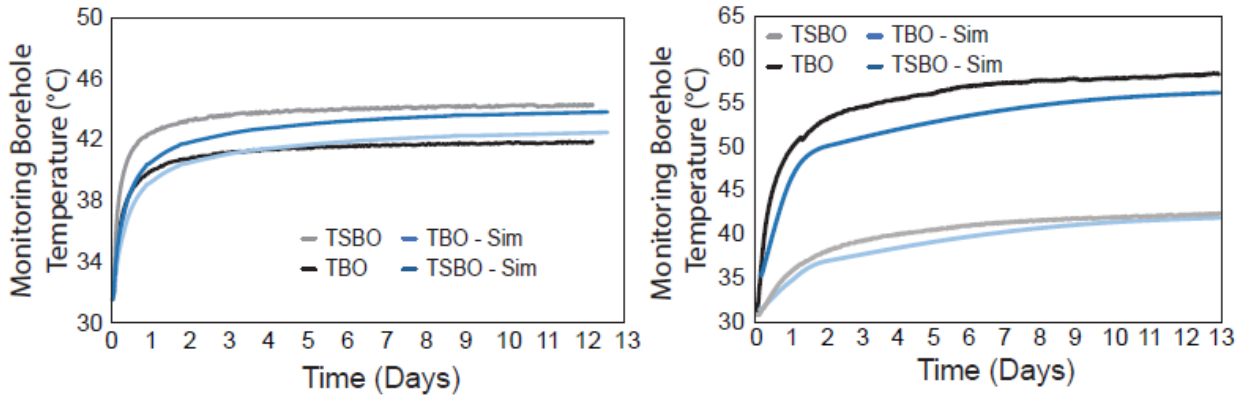


**Figure 4.5 A) Simulation of 260 W infrared heater and B) 750 W infrared heater experiment.**

The 750 W heater was placed deeper into the heated borehole causing the TSB temperature sensor to be out of plane with the heater. This reduces the temperature observed at TSB even though the overall energy flux into the formation was significantly higher. At the TB observation point, the temperature was raised approximately 28 °C, and in the salt adjacent to the heater, temperatures reached 144 °C. The successful simulation and implementation of the 750 W infrared heater experiment provides confidence in our ability to reach experimental design parameters during the Phase 1 experiments. With this heater achieving the desired temperatures the shakedown experiments were completed.

#### 4.1.4 Brine Availability

The results of 30 previous permeability experiments conducted at WIPP show that anhydrite permeability falls within the range  $9 \times 10^{-18}$  and  $2 \times 10^{-20}$  m<sup>2</sup> while halite permeability is between  $3 \times 10^{-16}$  to  $2 \times 10^{-23}$  m<sup>2</sup> [8]) During successive simulations we find that an initial permeability of  $10^{-21}$  m<sup>2</sup> for intact salt and  $10^{-18}$  for the borehole DRZ accurately reflects the water production during the shakedown experiments (Figure 4.6).

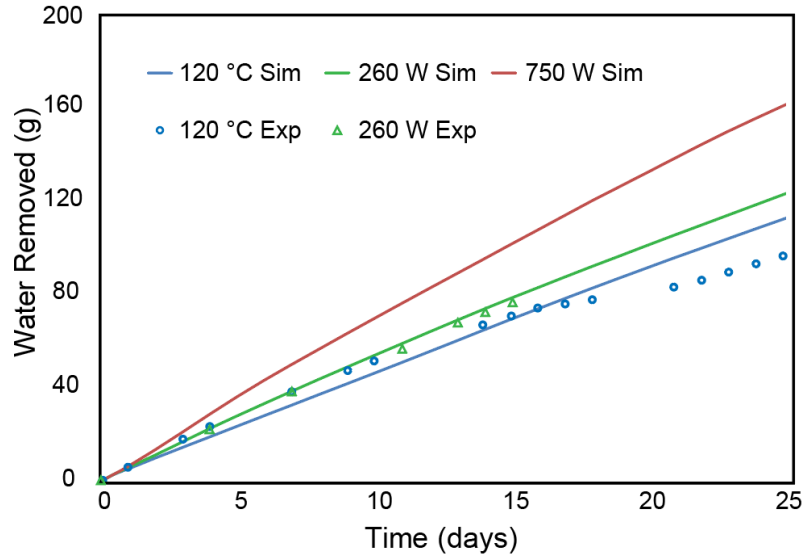


**Figure 4.6 Water production during the 120 °C heater block and 260 W radiative heating experiment compared to simulations. Observations from desiccant are points while the simulations are represented by lines.**

Due to the drying of the DRZ over the 6 years between when the borehole was drilled and testing began the water production from these tests is expected to be less than the water production from fresh boreholes. The simulation predicts that due to gravity the DRZ above the heater is approximately 38% saturated and the DRZ below the heater is approximately 50% saturated (Figure 4.7). The presence of this area of reduced saturation may serve to reduce the effects of thermal pressurization when heated. During heating the increased vapor pressure near the heater drives the remaining water out of the DRZ and to some extent the nearby intact salt. This results in increased water production with increased heat. Simulations suggest complete draining of the immediately adjacent DRZ happens quickly however draining the entire DRZ does not happen within 3 years of model simulation and will likely take many years.

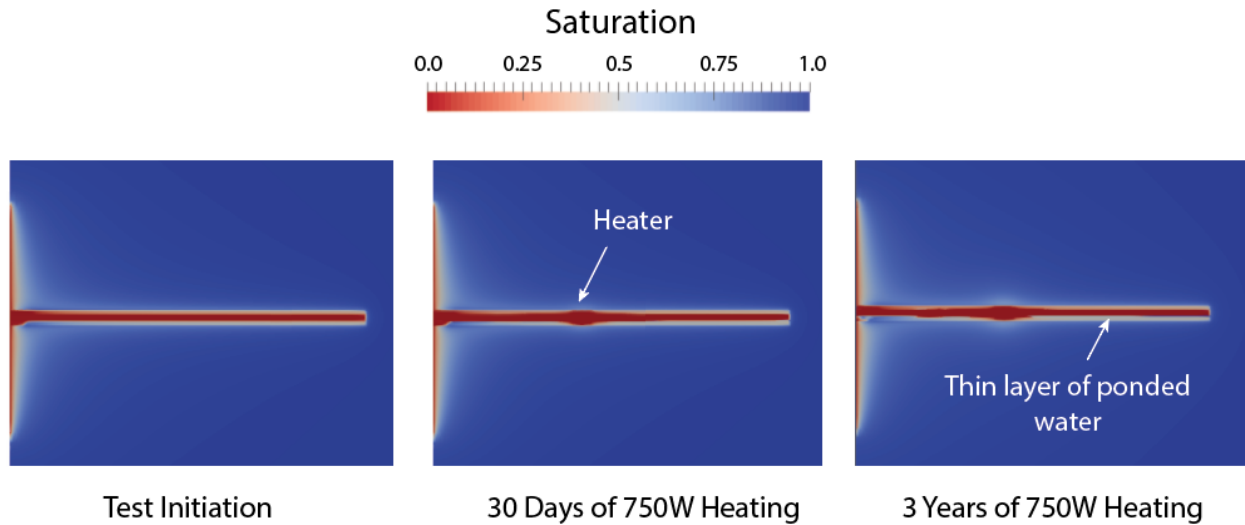


**Figure 4.7 Initial saturation condition at the start of testing, 30 days after 750 W radiative heating, and 3 years of 750 W heating. The heater increases the nearby vapor pressure and drives the remaining saturation out of the nearby DRZ and intact salt. After approximately 1 year water begins to pool behind the nitrogen injection.**

After approximately 1 year of simulation a thin layer of ponded water forms behind the nitrogen source and extends to the rear of the borehole (Figure 4.7). Once this ponded water approaches the nitrogen source the nitrogen humidity is increased and more water is produced. This changes the trend line from one where the only source of water is that which reaches the borehole between the packer and the nitrogen source to one where water is being sourced from the entire borehole behind the packer (Figure 4.8). This finding emphasizes the control that the size of the borehole and the location of the nitrogen injection has on the water produced. In general, longer boreholes will produce more water over time than shorter boreholes.

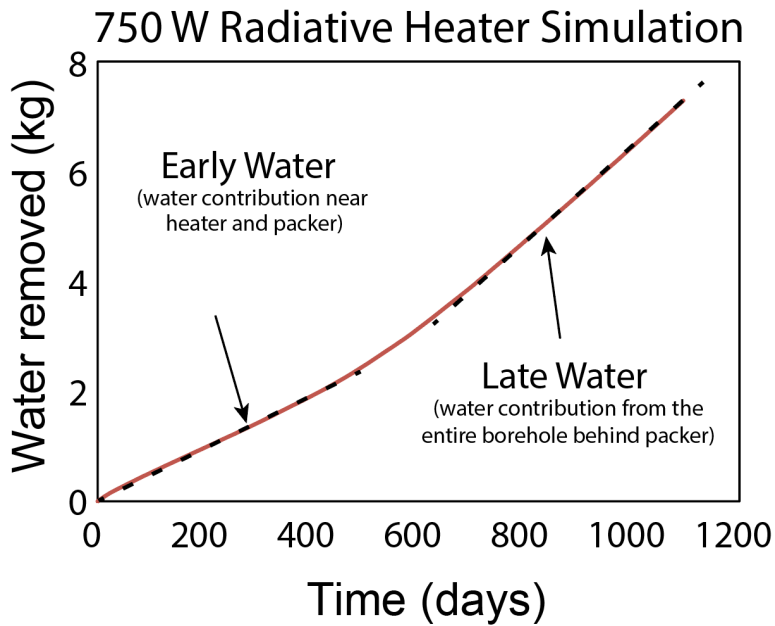


**Figure 4.8 Long term water production during a 750 W radiative heating simulation of the shakedown test. Two linear trends are identified: an early trend, which is controlled by water sourced between the heater and the nitrogen source, and a late trend, which receives water from the entire borehole through ponded water which accumulates and reaches the nitrogen source.**

During active waste emplacement of HLW, the DRZ around waste boreholes or newly excavated drifts may be completely saturated. Assuming the same conditions from the above simulations but with a completely saturated DRZ the models predict an additional inflow of 125 grams of water during the first year as additional water drains from the DRZ (Figure 4.9). These results are dependent on the size of the DRZ which is determined by the size of the excavation or borehole. However, it is likely that during actual waste emplacement activities, a portion of the initial increase in brine flow to the waste canisters could be avoided by constructing drifts and/or boreholes with a modest lead time.

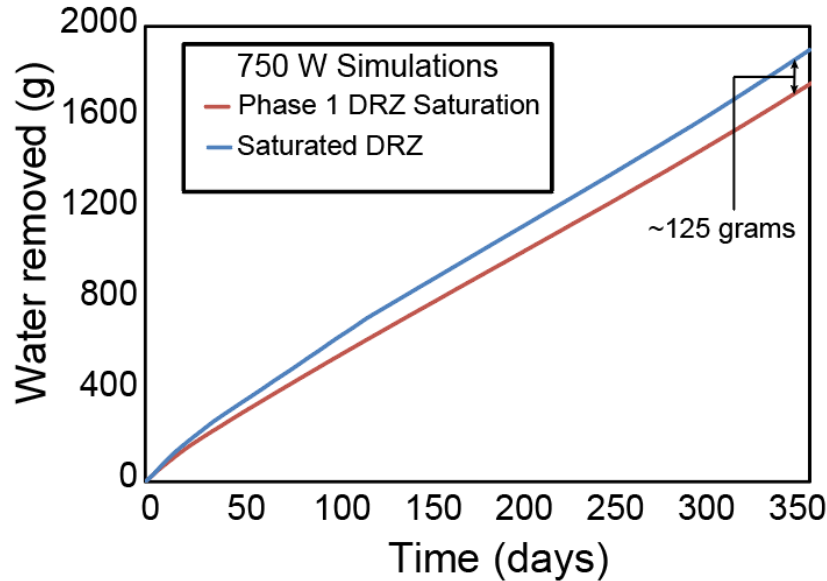


**Figure 4.9** A comparison of water production from a borehole with a saturated DRZ (freshly drilled) and one with the saturation profile of the shakedown simulation.

#### 4.1.5 Permeability Testing of Phase 2 Boreholes

During June 12<sup>th</sup> through 24<sup>th</sup> 2019, permeability testing was conducted on the freshly drilled Phase 1 boreholes as part of the preparation for beginning the larger scale experiment. While the permeability of intact salt is too low to measure without specialized equipment and procedures, the permeability of the DRZ around the boreholes can be significantly higher [8]. The goal of the permeability testing was twofold: (1) to identify the extent of the DRZ around the drift, and (2) to measure the permeability of the borehole DRZ. The general procedure included isolating a borehole section with an inflatable packer and then pressurizing the borehole behind the packer. Once pressurized the flow to borehole was stopped and the pressure decline was monitored with pressure transducers. 16 permeability tests were conducted at different depths and inflation pressures, within seven boreholes on the heated and unheated Phase 2 configurations (Table 4.2).

**Table 4.2 A summary of the permeability tests conducted on the Phase 1 borehole configurations**

Array	Borehole ID	Actual Depth, ft	Interval Tested, ft	Date
Heated	HP	12.23	9.03 to 12.23	6/12/2019
Heated	HP	12.23	9.06 to 12.23	6/13/2019
Heated	HP	12.23	9.06 to 12.23	6/18/2019
Heated	HP	12.23	9.06 to 12.23	6/18/2019
Heated	HP	12.23	7.03 to 12.23	6/18/2019
Heated	HP	12.23	5.03 to 12.23	6/18/2019
Heated	SL	8.08	5.03 to 8.08	6/18/2019
Heated	SL	8.08	5.03 to 8.08	6/19/2019
Heated	SM	15.01	5.00 to 15.01	6/19/2019
Heated	SM	15.01	7.00 to 15.01	6/19/2019
Heated	D	15	5.00 to 15.00	6/19/2019
Heated	D	15	5.00 to 15.00	6/19/2019
Unheated	HP	12.13	5.03 to 12.13	6/24/2019
Unheated	SL	8.05	5.03 to 8.05	6/24/2019
Unheated	D	15	5.00 to 15.00	6/24/2019
Unheated	D	15	7.00 to 15.00	6/24/2019

In general the drift DRZ was determined to extend approximately 4 to 5 feet in to the rock salt. Pressure tests less than 5 feet deep rapidly lost pressure. Gurgling sounds were noted during several tests which could be air escaping around the packer through fractures in the borehole DRZ. At times these gurgling sounds were lessened by increasing the inflation pressure within the packer. This could be due to the increased pressure from the packer closing off DRZ fractures or a poor packer seal in the borehole being corrected by high pressure. Several permeability tests were conducted in the HP borehole of the heated array where the Phase 1 packer will be placed. One such test, which did not gurgle and lost only a small amount of pressure is analyzed in Figure 4.10. FEHM simulations utilizing a 3 inch DRZ surrounding the HP borehole predict that the HP DRZ permeability is near  $2 \times 10^{-17} \text{ m}^2$  (Figure 4.10). This DRZ permeability falls within the range of  $3 \times 10^{-16}$  to  $2 \times 10^{-23} \text{ m}^2$  as reported by [8].

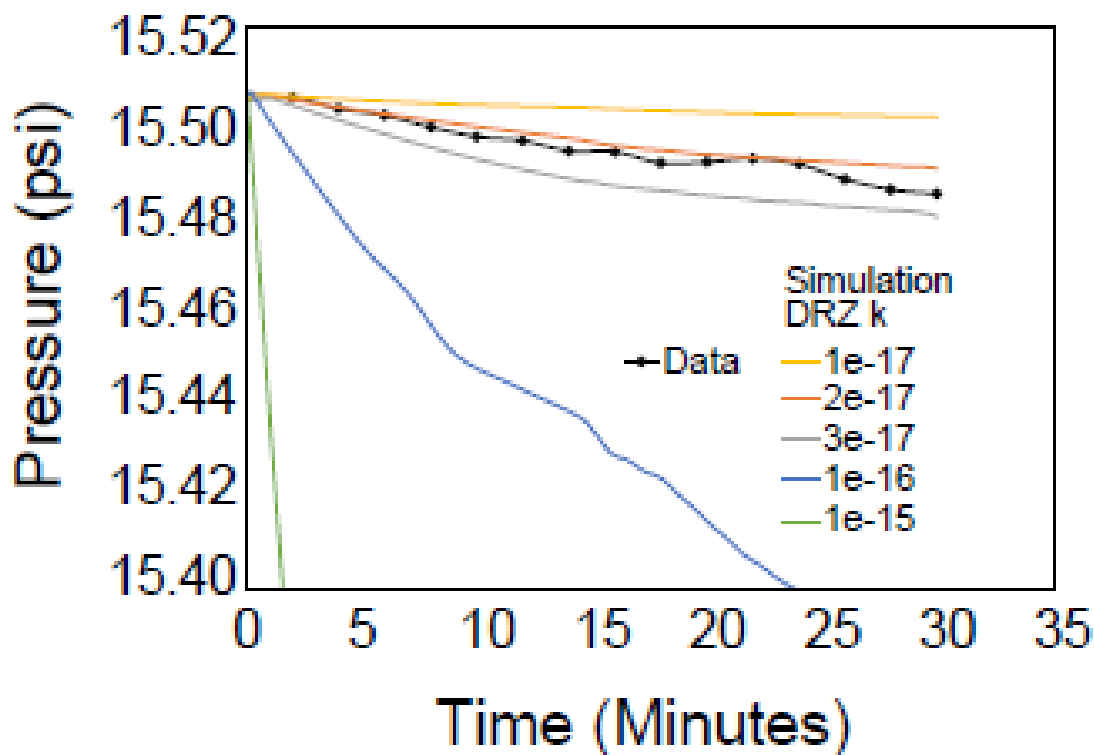
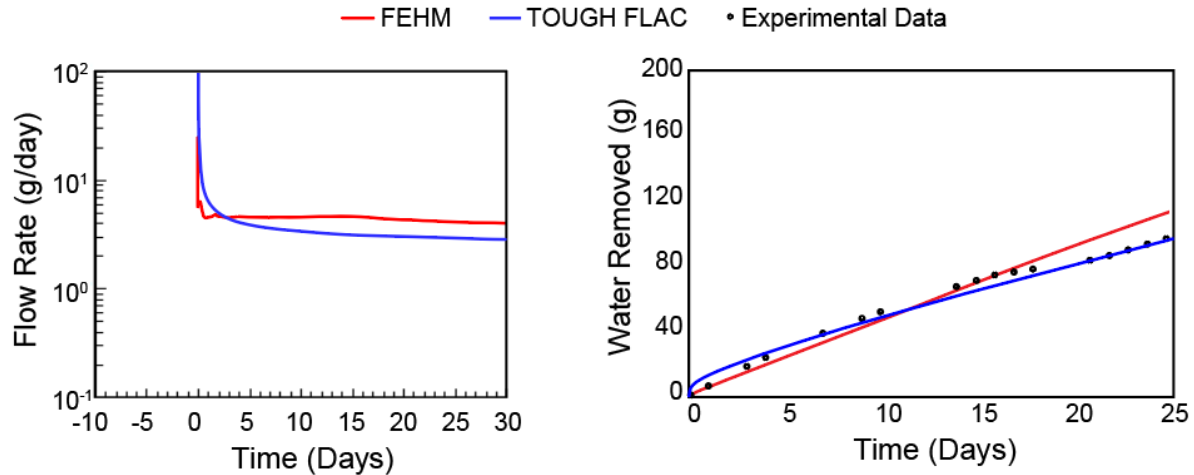


Figure 4.10 Permeability testing data compared to FEHM simulations of the heated borehole in the Phase 2 borehole configuration. The data is approximately matched with a permeability of  $2e-17 \text{ m}^2$ .

#### 4.2 TOUGH-FLAC coupled THM modeling of the shakedown test

Thermo-hydro-mechanical simulations of the shakedown test using TOUGH-FLAC have been carried out by LBNL [19]. The temperature profiles between the FEHM, TOUGH-FLAC, and experimental data are all in close agreement which increases our confidence in our ability to capture the temperature dependent thermal conductivity of the salt appropriately. The flow rate estimated for the  $120^\circ \text{C}$  steel block heater from the FEHM and TOUGH-FLAC simulations also agree but the FEHM simulations stabilize more quickly at a long term flow rate of approximately 5 grams/day while the TOUGH-FLAC simulations stabilize closer to 3 grams/day (Figure 4.11). Total water mass removal reflects the differences in flow rate, but overall both simulations produce a similar result.



**Figure 4.11 Comparison of flow rate predicted during the 120 C steel block heater predicted by FEHM (left) and TOUGH-FLAC (right). TOUGH-FLAC data from Rutqvist *et al.*, 2019.**

TOUGH-FLAC simulations include the creep closure of salt due to stress. These simulations predict only a small amount of closure during the 120° C heater block experiment. This is because of the small amount of heat transmitted into the salt. However, when exposed to a 750W radiative heater for 90 days the borehole closure will be almost 1 cm (Figure 4.12). During Phase 1 the closure of the borehole will be monitored and the simulations can be informed by the experimental results. Simulations comparing the larger scale Phase 2 experimental results to simulations using FEHM and TOUGH-FLAC will be reported in a future milestone.

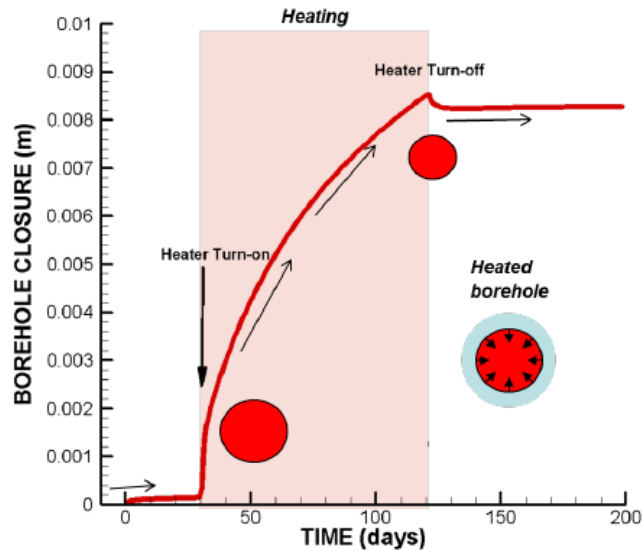


**Figure 4.12 Borehole closure due to 750W heating simulated using TOUGH-FLAC. Data from reference 19.**



## 5. Summary

The shakedown experiment was a heated borehole experiment conducted in the WIPP underground on pre-existing boreholes. The experiment included the use of several different heating regimes, temperature monitoring boreholes, and the monitoring of water production by the heated borehole. The shakedown experiment has proven very useful for testing equipment, developing numerical models, and working through the logistical challenges of working underground at WIPP. The implementation of a 750W radiative heater that reached a target temperature of 120° C in the nearby salt concluded the experiment. The selection of this heater demonstrates the benefit of an iterative design process which relied on “ground truthing” equipment along with predictive numerical modeling.

A heater mounted in a steel block is poorly suited to delivering energy into the salt formation due to poor thermal coupling, however, these experiments can be accurately modeled once an insulating air gap and radiative heat transfer are incorporated into FEHM. Radiative heaters deliver significantly more energy than conventional heater blocks and are capable of reproducing temperatures typical of spent fuel waste canisters. The successful simulation of the water production using an initial permeability of  $10^{-21}$  m<sup>2</sup> suggests the lack of a higher permeability clay layer within the shakedown boreholes, however, with limited high temperature experiments and a lack of isotopic and chemical testing of the brine it is difficult to discern the potential effect of mobilizing fluid inclusions. Including a damaged rock zone around the borehole within numerical simulations may be important for forecasting water production and thermal pressurization due to its potentially lower saturation, higher porosity and higher permeability. The extremely low permeability of salt means that the initial pressure and saturation condition of these experiments is not at steady state. Long term modeling can be used to develop the appropriate initial pressure and saturation distributions that account for the atmospheric pressure along the drift wall and boreholes. Good agreement on water production and thermal response from FEHM and TOUGH-FLAC give the team confidence in their ability to simulate the Phase 1 experiments. Data from the larger scale experiments will be used to refine these models further and explore the brine availability to spent fuel waste canisters in freshly drilled boreholes.

## 6. References

1. Bradshaw, R.L., and W.C. McClain. 1971. Project Salt Vault: A Demonstration of Disposal of High Activity Solidified Wastes in Underground Salt Mines. ORNL-4555. Oak Ridge, TN: Oak Ridge National Laboratory.
2. Brewitz, W., and T. Rothfuchs. 2007. “Concepts and Technologies for Radioactive Waste Disposal in Rock Salt.” *Acta Montani stica Slovaca Ročník 12 (1)* : 67–74.
3. Kühn, K. 1986. “Field Experiments in Salt Formations.” *Philosophical Transactions of the Royal Society of London A319*: 157–61.
4. Krause, W.B., and P.F. Gnirk. 1981. Domal Salt Brine Migration Experiments at Avery Island, Louisiana. 81-04. Rapid City: RESPEC, Inc.
5. Matalucci, R.V. 1987. In Situ Testing at the Waste Isolation Pilot Plant. SAND87-2382. Albuquerque: Sandia National Laboratories.

6. Nowak, E.J., D.F. McTigue, and R. Beraun. 1988. Brine Inflow to WIPP Disposal Rooms: Data, Modeling, and Assessment. SAND88-0112. Albuquerque: Sandia National Laboratories.
7. Wicks, G.G. 2001. "U.S. Field Testing Programs and Results." *Journal of Nuclear Materials* 298, 78–85.
8. Beauheim, R.L. & R.M. Roberts, 2002. Hydrology and hydraulic properties of a bedded evaporate formation, *Journal of Hydrology*, 259(1–4):66–68.
9. Beauheim, R.L., A. Ait-Chalal, G. Vouille, S.-M. Tijani, D.F. McTigue, C. Brun-Yaba, S.M. Hassanizadeh, G.M. van der Gissen, H. Holtman & P.N. Mollema, 1997. INTRAVAL Phase 2 WIPP 1 Test Case Report: Modeling of Brine Flow Through Halite at the Waste Isolation Pilot Plant Site. SAND97-0788. Albuquerque, NM: Sandia National Laboratories.
10. Caporuscio, F.A., Boukhalfa, H., Cheshire, M.C., Jorden, A.B., Ding, M. (2013) Brine Migration Studies for Salt Repositories. DOE Fuel Cycle Research and Development Document, FCRD-UFD-2013-000204
11. Carter, N.L., and Hansen, F.D. (1983) Creep of Rocksalt. *Tectonophysics*, V92, pp 275-333.
12. Kuhlman, K. L., Malama, B. 2013. Brine Flow in Heated Geologic Salt. SAND2013-1944. Sandia National Laboratories. Albuquerque, NM.
13. Boukhalfa, H., P.J. Johnson, D. Ware, D.J. Weaver, S. Otto, B.L. Dozier, P.H. Stauffer, M.M. Mills, E.N. Matteo, M.B. Nemer, C.G. Herrick, K.L. Kuhlman, Y. Wu & J. Rutqvist, 2018. Implementation of Small Diameter Borehole Thermal Experiments at WIPP. M3SF-18LA010303014, LA-UR-29203. Los Alamos, NM: Los Alamos National Laboratory.
14. Zyvoloski, G.A., B. A. Robinson, Z. V. Dash, S. Kelkar, H. S. Viswanathan, R. J. Pawar, P. H. Stauffer, T. A. Miller, S. P. Chu (2012), *Software users manual* (UM) for the FEHM Application Version 3.1-3.X, Los Alamos National Laboratory, Report: LA-UR-12-24493
15. Harp, D. R., P. H. Stauffer, P. K. Mishra, D. G. Levitt & B. A. Robinson (2014) *Thermal Modeling of High-Level Nuclear Waste Disposal in a Salt Repository*, *Nuclear Technology*, 187:3, 294-307, DOI: [10.13182/NT13-110](https://doi.org/10.13182/NT13-110)
16. Johnson, P. J., P. H. Stauffer, G. A. Zyvoloski, and S. M. Bourret (2018), *Experiments and Modeling to Support Field Test Design*, Los Alamos National Laboratory, Report: LA-UR-18-28189
17. Johnson, P. J., S. Otto, D. J. Weaver, B. Dozier, T. A. Miller, A. B. Jordan, N. G. Hayes-Rich, and P. H. Stauffer (2019), *Heat-Generating Nuclear Waste in Salt: Field Testing and Simulation*, *Vadose Zone Journal*, 18(1), doi: 10.2136/vzj2018.08.0160
18. Jordan, A.B., Boukhalfa, H., Caporuscio, F.A., Stauffer, P.H. *Brine Transport Experiments in Granular Salt* (2015), Los Alamos National Laboratory, Report: LA-UR-15-26804.
19. Rutqvist, J., W. Yuxin, H. Mengsu, C. Michael, W. Jiannan, and J. Birkholzer, 2019. *Salt Coupled THMC Processes Research Activities at LBNL : FY2019 Progress*, Lawrence Berkely National Laboratory, Report: LBNL-2001230.